Midkine promotes neuroblastoma through Notch2 signaling

Satoshi Kishida[1], Ping Mu[1], Shin Miyakawa[2], Masatoshi Fujiwara[2], Tomoyuki Abe[2], Kazuma Sakamoto[1], Akira Onishi[3], Yoshikazu Nakamura[2,4], Kenji Kadomatsu[1]

[1]Department of Biochemistry, Nagoya University Graduate School of Medicine, 65 Tsurumai-cho, Showa-ku, Nagoya 466-8550, Japan. [2]RIBOMIC, Inc., 3-16-13 Shirokanedai, Minato-ku, Tokyo 108-0071, Japan. [3]Transgenic Animal Research Center, National Institute of Agrobiological Sciences, 2 Ikenodai, Tsukuba 305-0901, Japan. [4]Department of Basic Medical Sciences, Institute of Medical Science, University of Tokyo, 4-6-1 Shirokanedai, Minato-ku, Tokyo 108-8639, Japan.

Running title: Midkine-Notch2 signaling in neuroblastoma

Keywords: Neuroblastoma, Midkine, Tumorigenesis, RNA aptamer, Molecular

therapy

Financial support:

This work was supported in part by a Grant-in-Aid for Cancer Research (20-13) from the Ministry of Health, Labour and Welfare (MHLW), Japan to K.K., a Grant-in-Aid from the National Cancer Center Research and Development Fund (22-4) to K.K., Grants-in-Aid (23110002, 23390078) from the Ministry of Education, Culture, Sports, Science and Technology (MEXT) of Japan to K.K., Grants-in-Aid (22790311, 24590377) from MEXT to S.K., a Grant-in-Aid from the Ministry of Agriculture, Forestry and Fisheries, Japan to K.K. and A.O., the funds from the Global COE program of MEXT, Japan to Nagoya University, Core Research for Evolution Science and Technology (CREST) grant from the Japan Science and Technology Agency to Y.N., and research grants to Y.N. from MEXT and MHLW.

Corresponding Author: Kenji Kadomatsu, Department of Biochemistry, Nagoya

University Graduate School of Medicine, 65 Tsurumai-cho, Showa-ku, Nagoya 466-8550, Japan. Phone: 81-52-744-2059; Fax: 81-52-744-2065; E-mail: kkadoma@med.nagoya-u.ac.jp

The authors disclose no potential conflicts of interest.

4944 words, 6 Figures and no table.

Abstract

Midkine (MK, MDK) is a heparin-binding growth factor highly expressed in various cancers, including neuroblastoma (NB), the most common extracranial pediatric solid tumor. Prognosis of NB patients where MYCN is amplified remains particularly poor. In this study, we employed a MYCN transgenic model for NB where MK is highly expressed in precancerous lesions of sympathetic ganglia. Genetic ablation of MK in this model delayed tumor formation and reduced tumor incidence. Furthermore, an RNA aptamer that specifically bound MK suppressed the growth of NB cells *in vitro* and *in vivo* in tumor xenografts. In precancerous lesions, MK-deficient MYCN Tg mice exhibited defects in activation of Notch2, a candidate MK receptor, and expression of the Notch target gene HES1. Similarly, RNA aptamer-treated tumor xenografts also showed attenuation of Notch2-HES1 signaling. Our findings establish a critical role for the MK-Notch2 signaling axis in NB tumorigenesis, which implicates new strategies to treat NB.

Introduction

Midkine (MK) is a heparin-binding growth factor originally identified in embryonal carcinoma cells, and has been implicated in tumor development (1-3). MK expression is intensive during the mid-gestation period and is decreased thereafter (4). Therefore MK expression is low in normal adult tissues. However it is resumed upon the development of various tumors, including Wilms' tumor (5), gastrointestinal cancer (6) and astrocytoma (7). In human colorectal cancer and prostate cancer, MK is strongly expressed at the precancerous stages (8, 9). Importantly, knockdown of MK in a xenograft model with colorectal and prostate cancer cells was associated with significant suppression of tumor growth (10-13). However, it remains elusive whether endogenous MK is crucial for tumorigenesis. Furthermore, reagents which block the function of secreted MK are still unavailable for clinical use.

Neuroblastoma (NB) is one of the cancers whose pathogenesis seems closely related to MK expression. NB, which arises from a neural crest-derived sympathetic neuronal lineage, is the most common extracranial pediatric solid

tumor (14). It accounts for around 15% of all pediatric cancer deaths, and the prognosis still remains poor in spite of an enormous amount of basic and clinical research. The transcription factor MYCN is one of the most potent predisposition genes for NB (14). There are several established prognostic factors for NB: MYCN amplification, low TRKA expression, diploidy and age older than 18 months have all been related with poor prognosis (15). In addition, we previously reported that MK could also be a potent prognostic factor (16, 17). MK mRNA is highly expressed in NB tissues with poor prognosis, whereas pleiotrophin (PTN), another family member of MK, is expressed in tumors with good prognosis (18).

As an animal model for NB, MYCN transgenic (Tg) mice, in which the human MYCN gene was integrated under the control of a rat tyrosine hydroxylase (TH) promoter, were generated (19). MYCN Tg mice spontaneously develop tumors mainly from the superior mesenteric ganglion (SMG), one of the sympathetic ganglia. Because those tumors are pathologically equivalent to human NB (19), they have been utilized for the molecular investigation of NB tumorigenesis. Hemizygous MYCN Tg mice show a hyperplasia phenotype in

the SMG at the age of 2 weeks, and these hyperplastic cells are thought to be precancerous lesions (20, 21).

RNA aptamers are biochemical or therapeutic agents that directly target a given molecule. An RNA aptamer which specifically recognizes a particular protein is selected from a complex library of random RNA sequences typically containing 10^{14} different molecules through a process known as SELEX (systematic evolution of ligands by exponential enrichment) (22-27). The concept is based on the ability of short (20-80-mer) RNA sequences to fold into unique 3-dimensional structures that recognize a particular target with high affinity and specificity. Therefore, aptamers can be thought of as nucleic acid analogs to antibodies.

In this study, we investigated the role of endogenous MK in the tumorigenesis of NB. In addition, we examined the therapeutic impact of an RNA aptamer that blocked secreted MK on NB in mice.

Materials and Methods

Cell culture

Human NB cell line TNB1, YT-nu and human prostate adenocarcinoma cell line LNCap were obtained from RIKEN Cell Bank (Tsukuba, Japan), the Carcinogenesis Division, National Cancer Center Research Institute (Tokyo, Japan) and American type culture collection, respectively. They were cultured with RPMI 1640 supplied with 10% heat-inactivated fetal bovine serum (FBS) in an incubator with humidified air at 37ºC with 5% CO_2. On receiving the cell lines, we prepared the frozen stocks within 1-2 passages. In every 1-2 months, we thawed the stock to keep original condition. They were routinely authenticated on the basis of viability, growth rate and morphology by microscopic examination.

Animals

MYCN Tg mice (19) were maintained in our animal facility under a controlled environment and provided with standard nourishment and water. They were crossed with 129^{+Ter}/SvJcl wild-type mice (CLEA Japan). Their abdomens

were inspected for the tumor every week, and mice with the tumor were immediately euthanized with CO_2. MK-knockout mice were established as previously described (28). This study was approved by the Animal Care and Use Committee of Nagoya University Graduate School of Medicine.

RT-PCR and Real-time PCR

RNA extraction from SMG, tumor tissues and cultured cells, and RT-PCR were carried out as previously described (29). The annealing temperatures and primer sequences for each gene were shown in Supplementary Table S1. Real-time PCR for MK was carried out with TaqMan Gene Expression Assays (ABI) and an Mx3005P Real-time QPCR System (Agilent). The assay IDs for MK and GAPDH are Mm00440279_m1 and Mm03302249_g1, respectively. For HES1, RT and real-time PCR were carried out with ReverTra Ace (TOYOBO) and KAPA SYBR FAST Universal qPCR Kit (KAPA BIOSYSTEMS), respectively. The relative expression levels were acquired according to the manufacturer's instructions ($\Delta\Delta$Ct method).

Immunohistochemistry

Immunohistochemistry was carried out as previously described (29) using following primary antibodies: rabbit anti-MK (raised against recombinant full-length mouse MK, 1:1000), mouse anti-MYCN (OP13, 1:20; Calbiochem), mouse anti-Ki-67 (550609, 1:20; BD Biosciences), rabbit anti-TH (AB152, 1:100; Chemicon), rabbit anti-Notch2 FL (07-1233, 1:100; Millipore), rabbit anti-Notch2 ICD (07-1234, 1:100; Millipore) and rabbit anti-HES1 (AB5702, 1:100; Millipore). Biotin Goat Anti-Rabbit Ig (550338, 1:10; BD Biosciences) and Biotin Goat Anti-Mouse Ig (550337, 1:50; BD Biosciences) were used as secondary antibodies. The signals were visualized with a VECTASTAIN Elite ABC standard Kit (Vector Laboratories) and DAB (K3468, DAKO), and counterstained with hematoxylin.

Western blotting

Protein extraction from tumor tissues and cultured cells, and Western blotting were carried out as previously described (29). For the detection of MK in medium, cultured cells in a 6-well dish were exposed to serum-free medium containing 20 μg/ml of heparin sodium salt. 12 hours later, the media were

harvested and the cells were washed with PBS. MK is easily attached to the cell surface or extracellular matrix. When we detect the secreted MK level, we usually add heparin because MK possesses strong affinity to heparin, and heparin-bound MK is kept in the medium. For the detection of Notch2 (ICD), cultured cells and tumor tissues were suspended in low-salt buffer (10mM HEPES-KOH pH 7.8, 10mM KCl, 0.1mM EDTA, 0.25% NP-40, protease inhibitor cocktail and phosphatase inhibitor cocktail (Nacalai Tesque, Japan)), and homogenized on ice with dounce homogenizer. After the centrifuge (4000 rpm, 5 minutes), the supernatants were mixed with sample buffer (cytosol and membrane extract). The pellets were homogenized with low-salt buffer again, and sonicated in RIPA buffer (nucleus extract). Protein amounts were quantified (BCA Protein Assay Kit, Thermo), and subjected to SDS-PAGE. The following primary antibodies were used: goat anti-human MK (1:1000) (30), mouse anti-β-actin (A5441, 1:1000; Sigma), rabbit anti-ALK (3333, 1:1000; Cell Signaling), rabbit anti-Phospho-ALK (3341, 1:1000; Cell Signaling), rabbit anti-Histone H3 (9715, 1:1000; Cell Signaling). Antibody against Notch2 (ICD)

was the same as that for IHC (1:1000).

RNA aptamers

An RNA aptamer to MK (77 nucleotides length) was selected by SELEX (23-25). 2'-fluoro modified pyrimidines were used for nuclease resistance. This aptamer was truncated to 40 nucleotides and was partially modified with 2'-O-methyl modification (Apt-1). Apt-1 was chemically synthesized with an RNA synthesizer (Gene Design). As a negative control, an RNA, which was composed of scramble sequences of Apt-1 and had much lower affinity to MK, was also chemically synthesized (Apt-nc).

Surface plasmon resonance (SPR) assay

SPR assays were carried out as previously described using a BIAcore T100 instrument (GE Healthcare) (23). The 3'-biotinylated Apt-1 and negative control RNA (Apt-nc) were immobilized on the flow cell 2 and 3 of a SA sensor chip, respectively. The resonance units (RU) of these immobilized oligonucleotides were about 270. Human MK (Peptide Institute Inc.), human PTN (Peptide Institute Inc.), human IgG1 (Calbiochem) and human albumin

(Sigma) were dissolved in the running buffer with 0.5 g/L transfer RNA (Sigma). The final concentrations were 100 nM. The running buffer was a mixture of 145 mM NaCl, 5.4 mM KCl, 1.8 mM $CaCl_2$, 0.8 mM $MgCl_2$, 20 mM pH 7.6 Tris-HCl and 0.05% Tween 20.

AP assay

The cDNA for human MK coding the region from Lys23 to the stop codon was cloned into an APtag-5 vector utilizing XhoI and XbaI sites. 293T cells were plated onto a 10 cm dish ($2.0x10^6$ cells/dish). The next day, 293T cells were transfected with APtag-5 or APtag-5-MK vector using FuGENE6 (Roche). 5 days later, the media were harvested and filtered through a 0.22 μm PES membrane. The collected AP proteins were kept at 4ºC. For *in vitro* assay, TNB1 cells ($0.1x10^6$ cells/well) were plated in 6-well dishes coated with collagen I. 24 hours later, the cells were washed with HBHA (HBSS with 0.5 mg/ml BSA, 20 mM HEPES pH 7.0) and incubated with 1 U/ml of AP or AP-MK and 100 nM of each aptamer for 90 minutes at room temperature. Then the cells were washed 5 times with HBHA and lysed with 200 μl of cell lysis buffer (Q504, GenHunter).

Endogenous AP was inactivated at 65ºC for 10 minutes. 50 μl of the cell lysate was mixed with an equal volume of AP Assay Reagent A (Q501, GenHunter), and incubated at 37ºC for 15 minutes. 100 μl of 0.5 M NaOH was added to stop the reaction, and the $O.D._{405}$ value was measured to calculate the AP activity according to the instructions from GenHunter (31, 32).

Soft agar assay

1.5 ml of bottom agar (0.5% agar/RPMI + 10% FBS) was plated on 6-well dishes (n=3). 1 ml of top agar (0.33% agar/RPMI + 10% FBS) containing TNB1 cells (2000 cells/well), YT-nu cells (2000 cells/well) or LNCap cells (5000 cells/well) with or without 100 nM of each aptamer and 100 ng/ml of recombinant human MK (R&D, 258-MD) was plated on the bottom agar. On the next day, 1 ml of serum-free RPMI was added to each well. Two weeks later, the colonies were stained with crystal violet and counted (6 fields/well).

Therapeutic experiments using a xenograft model in nude mice

TNB1 cells ($5x10^6$ cells in 50% Matrigel; BD Biosciences) or YT-nu cells ($1x10^7$ cells in 50% Matrigel) were subcutaneously inoculated into the left

and right flank of 8-week-old athymic nude mice (KSN/Slc; SLC, Japan). One week later, when the tumors reached a volume of approximately 50–80 mm^3, the mice were randomly divided into groups (n=4 each). 100 μg/tumor of each aptamer was intratumorally administrated twice per week, and tumor volumes were calculated with the following formula: volume [mm^3] = $(width)^2$ x length/2 (33).

Statistical analysis

Results are presented as the mean ± SD. Their homoscedasticities were checked by f-test. Statistical significance was evaluated with a two-tailed, unpaired t-test. In Fig. S8C, Welch's correction was applied.

Results

MK is expressed in the precancerous lesions of MYCN Tg mice

At 2 weeks of age, while the SMG in wild-type mice consisted of fully differentiated ganglion cells, undifferentiated neuroblasts (small round cells) were locally accumulated in the SMG of MYCN Tg mice; these cells are collectively referred to as a hyperplasia (Fig. 1A, arrowheads). These observations were consistent with previous reports (20, 21, 29). Although the SMG in wild-type mice expressed a low level of MK mRNA, the level was significantly increased in MYCN Tg mice (Fig. 1B). Quantitative real-time PCR showed that MK mRNA was upregulated approximately 5-fold in MYCN Tg mice (Fig. 1C). Other MK-related genes were also examined (Fig. 1B and Supplementary Fig. S1). Notch2 (34, 35), LRP1 (36-38), PTPζ (39) and Integrins (α4, α6, β1) (40) are candidates for MK receptors, and they were similarly expressed in both wild-type and MYCN Tg mice. ALK is another receptor candidate (41). Interestingly, ALK mRNA was dominantly expressed in MYCN Tg mice (Fig. 1B). PTN is the only family member of MK. In contrast to MK, the PTN

expressions were constant between wild-type and MYCN Tg mice (Fig. 1B).

Immunohistochemical staining also revealed that the MK protein was intensively expressed in hyperplasia lesions (Fig. 1D). Neuroblasts in hyperplasia lesions strongly expressed the transgene MYCN and the proliferation marker Ki-67, and were negative for the differentiation marker TH (Fig. 1E), as previously reported (20, 42). Taken together, these results showed that MK was highly expressed in precancerous hyper-proliferative cells. Furthermore, MK and the related genes were continuously expressed in the growing tumor (Supplementary Fig. S2).

The suppression of tumor incidence and progression in MK-knockout mice

Next we addressed the involvement of endogenous MK for the tumorigenesis of MYCN Tg mice. To this end, we crossed the MK-knockout mice with MYCN Tg mice, and monitored their phenotype. As shown in Fig. 2A, MYCN Tg mice (hemizygotes) began to die from 6 weeks of age, and the peak of the deaths from tumor occurred at an age of 9 to 14 weeks. As a result, around 30% of MYCN Tg mice were free of tumor. On the other hand, MYCN Tg

mice possessing homozygous deletion of the MK gene ($MK^{-/-}$) exhibited the suppressed phenotype (Fig. 2A). Their tumor deaths were delayed for 1-2 weeks and more than 40% of them were tumor-free. $MK^{+/-}$ mice expressed significantly lower levels of MK proteins compared to $MK^{+/+}$ mice, but still expressed some (Fig. 2B). The survival curve of $MK^{+/-}$ mice was intermediate between those of $MK^{+/+}$ and $MK^{-/-}$ mice. Taken together, our data suggested that MK is involved in the tumor incidence and progression of MYCN Tg mice.

Attenuation of Notch2 activity in the precancerous lesions of MK-deficient mice

Recently, MK-Notch2 signaling in pancreatic cancer was reported (35). Because MK-knockout mice showed a tumor-suppressive phenotype (Fig. 2A), we examined whether Notch2 activity was attenuated in these mice. The full-length (FL) and the intracellular domain (ICD) of Notch2, an active form which translocates into the nucleus, were immunostained to evaluate the activation of Notch2 in the SMG of 2-week-old precancerous mice. $MK^{+/+}$ mice showed both FL and ICD staining at the hyperplasia lesion (Fig. 3A, B), which

indicates the activation of Notch2 signaling. In contrast, although FL was also expressed in $MK^{-/-}$ mice (Fig. 3D), ICD staining was markedly diminished compared to $MK^{+/+}$ mice (Fig. 3E). In addition, the expression of HES1, one of the major target genes of Notch, was also decreased in $MK^{-/-}$ mice (Fig. 3C, F). These results indicate the attenuation of the Notch2 signal in $MK^{-/-}$ mice, and strongly suggest the possibility that MK signals via Notch2 to regulate early tumorigenesis in MYCN Tg mice.

An RNA aptamer targeting MK inhibits its binding to the cell surface

For the purpose of targeting MK protein, we selected RNA aptamers to MK from a complex library of random RNA sequences through the SELEX process. The initial isolates of anti-MK aptamers contained several variants of distinct properties. Of these, we isolated the MK-specific aptamer designated as Apt-1. In addition, we synthesized a scrambled negative control, Apt-nc. SPR analysis indicated that Apt-1 specifically recognized MK, but not PTN and other plasma proteins (Fig. 4A, Supplementary Fig. S3). In order to examine whether Apt-1 could block the binding of MK to the cell surface *in vitro*, we utilized an

alkaline phosphatase (AP) assay system (31, 32). We constructed a secreted AP-MK fusion protein-expressing plasmid, and collected AP-MK proteins secreted from transfected 293T cells (Fig. 4B). AP-MK proteins were added to the NB cell line TNB1 expressing endogenous MK (Fig. 5C), and AP activity bound to the cell surface was measured. In the presence of Apt-1, AP-MK binding to the surface of TNB1 cells was significantly blocked, but Apt-nc showed no effect (Fig. 4C, Supplementary Fig. S4). These results indicate that Apt-1 exerts a specific and effective activity to block MK binding to the cell surface.

The RNA aptamer Apt-1 suppressed the growth of NB cells both in vitro and in vivo

Consistent with its activity to block the binding of MK to the cell surface, Apt-1 treatment slightly suppressed the production of Notch2 (ICD) (Fig. 4D), and significantly reduced the expression of HES1 mRNA in TNB1 cells (Fig. 4E). Next we evaluated the anchorage-independent colony formation of TNB1 cells. TNB1 cells were cultured in soft agar plates in the absence or presence of RNA

aptamers. As a result, the addition of Apt-1 effectively blocked the colony formation in soft agar (Fig. 5A) (Supplementary Fig. S5). In contrast, Apt-nc showed no inhibitory effects. The same results were observed in another NB cell line, YT-nu (Supplementary Fig. S7A). Importantly, the addition of recombinant MK protein could cancel the inhibitory effect of Apt-1 (Fig. 5A) (Supplementary Fig. S7A). In contrast, Apt-1 showed no effect on LNCap cells, a prostate adenocarcinoma cell line, which expressed little MK (Fig. 5B, C). These results strongly ensure the specificity of Apt-1. We also examined the *in vivo* therapeutic effect using a xenograft model with TNB1 cells. We carried out intratumor injections of Apt-1 to engrafted subcutaneous tumors twice per week (100 μg each) (Fig. 5D). Although Apt-nc showed no significant effects, Apt-1 injection revealed marked suppression of tumor growth in terms of both tumor volume and weight (Fig. 5E, F, Supplementary Fig. S6). We confirmed the same results with YT-nu cells (Supplementary Fig. S7B-E). As a result, the RNA aptamer Apt-1 turned out to have specific and efficient activity to block MK function and suppress tumor growth *in vivo*.

Notch2 signaling was suppressed in Apt-1-treated tumors

In order to confirm the effect of Apt-1, we investigated the Notch2 signaling in Apt-1-treated xenograft tumors. Immunohistochemistry (Fig. 6A) and Western blotting (Fig. 6B) demonstrated that Notcn2 (ICD) levels were suppressed in Apt-1-treated tumors. In addition, the expression of HES1 protein (Fig. 6A) and mRNA (Fig. 6C) were significantly decreased in Apt-1-treated tumors. In contrast, Apt-1 exerted no obvious inhibitory effect on ALK activation (Fig. 6B). We confirmed the same results with Apt-1-treated YT-nu xenograft tumors (Supplementary Fig. S8). Taken together, these results suggest that the anti-tumor effect of Apt-1 should be mediated by the inhibition of MK-Notch2 axis.

Discussion

Here we have shown that endogenous MK is involved in the tumorigenesis of NB in MYCN Tg mice. At the age of 2 weeks, MYCN Tg mice showed the hyperplasia phenotype in the SMG, in which undifferentiated neuroblasts were locally accumulated (Fig. 1A). Although all MYCN Tg mice at 2 weeks of age showed the hyperplasia status, only around 70% of them developed NB afterward (Fig. 2A). These results indicate that the SMG at 2 weeks of age would not be completely tumorigenic. We found that MK was more highly expressed at those hyperplasia lesions than in the surrounding differentiated ganglion cells (Fig. 1B-D). Furthermore, MK deficiency suppressed the tumor incidence and growth rate in MYCN Tg mice (Fig. 2), which supports the idea that MK is involved in the tumorigenesis of NB. PTN is the only family member of MK. In terms of the relationship between their expression levels and prognoses, MK and PTN show opposite profiles. That is, high MK and low PTN expressions are related to poor prognosis (18). In contrast to MK, PTN was equally expressed in the 2-week SMG of MYCN Tg and wild-type mice (Fig. 1B).

Therefore, in spite of the structural similarity, PTN might not be involved in the tumorigenesis of NB in MYCN Tg mice.

The tumor incidence observed in MYCN Tg mice was suppressed in MK-deficient mice (Fig. 2A). Moreover, Apt-1-mediated targeting of MK in xenograft model revealed an outstanding tumor-suppressive effect (Fig. 5, Supplementary Fig. S6 and S7). But, there is a difference between MK-deficient mice and xenograft model in terms of the effectiveness of MK targeting. As MYCN Tg mice undergo severe chromosomal aberrations (19), some compensatory events might happen during the tumorigenesis of MK deficient mice. On the other hand, since normal ($MK^{+/+}$) NB cells keep secreting MK and proliferating, they could be addicted to MK signaling and could show the sensitive response to Apt-1 treatment.

We utilized the RNA aptamer to target MK. It is important to note that RNA aptamers are considered to be highly potential therapeutics. Indeed, anti-vascular endothelial growth factor aptamer, Macugen, is in market for curing age-related macular degeneration, and other 9 programs are now in clinical

studies (43, 44). The SPR study showed that Apt-1 could bind to MK much more strongly than PTN and other plasma proteins (Fig. 4A, Supplementary Fig. S3), suggesting that Apt-1 could specifically bind to MK in physiological conditions. Intratumor administration of Apt-1 dramatically suppressed the growth of a subcutaneous tumor derived from TNB1 (Fig. 5) or YT-nu cells (Supplementary Fig. S7). Since RNA aptamers chemically modified to improve their pharmacokinetics can be applied for systemic administration (26), they could be efficient tools to target MK in NB patients with an unfavorable prognosis.

So far, the intracellular signaling pathway activated by MK has not been fully elucidated. Among the candidates for its receptor, ALK has a close relation to the pathogenesis of NB. Thus, ALK has been shown to be the predisposition gene for familial NB, and it is also somatically mutated and hyper-activated in some NB patients (45-48). Interestingly, ALK is the only receptor candidate showing the dominant expression in the precancerous SMG of MYCN Tg mice (Fig. 1B, Supplementary Fig. S1). This might suggest that MK and ALK function cooperatively during the tumorigenesis of NB. However, we also found that Apt-1

could efficiently suppress the growth of xenograft tumor derived from TNB1 cells (Fig. 5). TNB1 cells possess the R1275Q mutation, one of the most common hyperactive mutations in the ALK gene. Our data suggest that MK functions independently of ALK in terms of the regulation of tumorigenesis. Consistent with this, the knockdown of MK with shRNA can suppress the growth of SH-SY5Y cells, an NB cell line possessing another hyperactive mutation (F1174L) in the ALK gene (data not shown).

Based on these observations, we speculate that a receptor other than ALK is vital for MK signaling in the tumorigenesis of NB. In this context, our finding on Notch2 is interesting. Recently, it has been reported that Notch2 acts as a functional receptor of MK in pancreatic cancer, and MK-Notch2 signaling regulates the epithelial-mesenchymal transition and chemotherapy resistance (35). Notch signaling is involved in the early development of the neural crest (49). The tumorigenesis of NB and the development of neural crest-derived cells may share some molecular mechanisms. Here we found that MK deficiency resulted in attenuated Notch2 activation in the hyperplasia lesions of the SMG in

2-week-old MYCN Tg mice (Fig. 3). This is the first physiological data *in vivo* suggesting the involvement of MK in a particular type of receptor signaling. Recently, it has been reported that MK and ALK were cooperatively involved in the normal development of chicken sympathetic neurons (50). Our current results indicate that Notch2 should function as a MK receptor during the tumorigenesis of NB. However, these two studies do not exclude the possibility that there is a functional relationship between the MK-ALK and MK-Notch2 pathways. This issue should be verified in the future study. Finally, in order to unveil the molecular mechanism by which MK-Notch2 signaling regulates the pathogenesis of NB, the identification of target genes other than HES1 should be a future topic of research.

Acknowledgments

We thank Dr. Makoto Sawada and Dr. Kenji Ono, Department of Brain Functions, Division of Stress Adaptation and Protection, Research Institute of Environmental Medicine, Nagoya University, for the use of MRI equipment. We

also thank Misako Tanase for her technical assistance, and members of RIBOMIC Inc. for discussion.

References

1. Kadomatsu K, Tomomura M, Muramatsu T. cDNA cloning and sequencing of a new gene intensely expressed in early differentiation stages of embryonal carcinoma cells and in mid-gestation period of mouse embryogenesis. Biochem Biophys Res Commun 1988;151:1312-8.

2. Tomomura M, Kadomatsu K, Nakamoto M, Muramatsu H, Kondoh H, et al. A retinoic acid responsive gene, MK, produces a secreted protein with heparin binding activity. Biochem Biophys Res Commun 1990;171:603-9.

3. Kadomatsu K, Muramatsu T. Midkine and pleiotrophin in neural development and cancer. Cancer Lett 2004;204:127-43.

4. Kadomatsu K, Huang RP, Suganuma T, Murata F, Muramatsu T. A retinoic acid responsive gene MK found in the teratocarcinoma system is expressed in spatially and temporally controlled manner during mouse embryogenesis. J Cell Biol 1990;110:607-16.

5. Tsutsui J, Kadomatsu K, Matsubara S, Nakagawara A, Hamanoue M, et al. A new family of heparin-binding growth/differentiation factors: increased midkine

expression in Wilms' tumor and other human carcinomas. Cancer Res 1993;53:1281-5.

6. Aridome K, Tsutsui J, Takao S, Kadomatsu K, Ozawa M, Aikou T, et al. Increased midkine gene expression in human gastrointestinal cancers. Cancer Res 1995;86:655-61.

7. Mishima K, Asai A, Kadomatsu K, Ino Y, Nomura K, Narita Y, et al. Increased expression of midkine during the progression of human astrocytomas. Neurosci Lett 1997;233:29-32.

8. Ye C, Qi M, Fan QW, Ito K, Akiyama S, et al. Expression of midkine in the early stage of carcinogenesis in human colorectal cancer. Br J Cancer 1999;79:179-84.

9. Konishi N, Nakamura M, Nakaoka S, Hiasa Y, Cho M, Uemura H, et al. Immunohistochemical analysis of midkine expression in human prostate carcinoma. Oncology 1999;57:253-7.

10. Takei Y, Kadomatsu K, Matsuo S, Itoh H, Nakazawa K, Kubota S, et al. Antisense oligodeoxynucleotide targeted to Midkine, a heparin-binding growth

factor, suppresses tumorigenicity of mouse rectal carcinoma cells. Cancer Res 2001;61:8486-91.

11. Takei Y, Kadomatsu K, Itoh H, Sato W, Nakazawa K, Kubota S, et al. 5'-,3'-inverted thymidine-modified antisense oligodeoxynucleotide targeting midkine. Its design and application for cancer therapy. J Biol Chem 2002;277:23800-6.

12. Takei Y, Kadomatsu K, Yuasa K, Sato W, Muramatsu T. Morpholino antisense oligomer targeting human midkine: its application for cancer therapy. Int J Cancer 2005;114:490-7.

13. Takei Y, Kadomatsu K, Goto T, Muramatsu T. Combinational antitumor effect of siRNA against midkine and paclitaxel on growth of human prostate cancer xenografts. Cancer 2006;107:864-73.

14. Nakagawara A, Ohira M. Comprehensive genomics linking between neural development and cancer: neuroblastoma as a model. Cancer Lett 2004;204:213-24.

15. Maris JM, Hogarty MD, Bagatell R, Cohn SL. Neuroblastoma. Lancet 2007;369:2106-20.

16. Ikematsu S, Nakagawara A, Nakamura Y, Sakuma S, Wakai K, Muramatsu T, et al. Correlation of elevated level of blood midkine with poor prognostic factors of human neuroblastomas. Br J Cancer 2003;88:1522-6.

17. Ikematsu S, Nakagawara A, Nakamura Y, Ohira M, Shinjo M, Kishida S, et al. Plasma midkine level is a prognostic factor for human neuroblastoma. Cancer Sci 2008;99:2070-4.

18. Nakagawara A, Milbrandt J, Muramatsu T, Deuel TF, Zhao H, Cnaan A, et al. Differential expression of pleiotrophin and midkine in advanced neuroblastomas. Cancer Res 1995;55:1792-7.

19. Weiss WA, Aldape K, Mohapatra G, Feuerstein BG, Bishop JM. Targeted expression of MYCN causes neuroblastoma in transgenic mice. EMBO J 1997;16:2985-95.

20. Hansford LM, Thomas WD, Keating JM, Burkhart CA, Peaston AE, Norris MD, et al. Mechanisms of embryonal tumor initiation: distinct roles for MycN

expression and MYCN amplification. Proc Natl Acad Sci U S A 2004;101:12664-9.

21. Huang P, Kishida S, Cao D, Murakami-Tonami Y, Mu P, Nakaguro M, et al. The neuronal differentiation factor NeuroD1 downregulates the neuronal repellent factor Slit2 expression and promotes cell motility and tumor formation of neuroblastoma. Cancer Res 2011;71:2938-48.

22. Oguro A, Ohtsu T, Svitkin YV, Sonenberg N, Nakamura Y. RNA aptamers to initiation factor 4A helicase hinder cap-dependent translation by blocking ATP hydrolysis. RNA 2003;9:394-407.

23. Miyakawa S, Oguro A, Ohtsu T, Imataka H, Sonenberg N, Nakamura Y. RNA aptamers to mammalian initiation factor 4G inhibit cap-dependent translation by blocking the formation of initiation factor complexes. RNA 2006;12:1825-34.

24. Keefe AD, Schaub RG. Aptamers as candidate therapeutics for cardiovascular indications. Curr Opin Pharmacol 2008;8:147-52.

25. Miyakawa S, Nomura Y, Sakamoto T, Yamaguchi Y, Kato K, Yamazaki S, et al. Structural and molecular basis for hyperspecificity of RNA aptamer to human immunoglobulin G. RNA 2008;14:1154-63.

26. Ishiguro A, Akiyama T, Adachi H, Inoue J, Nakamura Y. Therapeutic potential of anti-interleukin-17A aptamer: suppression of interleukin-17A signaling and attenuation of autoimmunity in two mouse models. Arthritis Rheum 2011;63:455-66.

27. Adachi H, Ishiguro A, Hamada M, Sakota E, Asai K, Nakamura Y. Antagonistic RNA aptamer specific to a heterodimeric form of human interleukin-17A/F. Biochimie 2011;93:1081-8.

28. Nakamura E, Kadomatsu K, Yuasa S, Muramatsu H, Mamiya T, Nabeshima T, et al. Disruption of the midkine gene (Mdk) resulted in altered expression of a calcium binding protein in the hippocampus of infant mice and their abnormal behaviour. Genes Cells 1998;3:811-22.

29. Asano Y, Kishida S, Mu P, Sakamoto K, Murohara T, Kadomatsu K. DRR1 is expressed in the developing nervous system and downregulated during

neuroblastoma carcinogenesis. Biochem Biophys Res Commun 2010;394:829-35.

30. Maehara H, Kaname T, Yanagi K, Hanzawa H, Owan I, Kinjou T, et al. Midkine as a novel target for antibody therapy in osteosarcoma. Biochem Biophys Res Commun 2007;358:757-62.

31. Flanagan JG, Cheng HJ, Feldheim DA, Hattori M, Lu Q, Vanderhaeghen P. Alkaline phosphatase fusions of ligands or receptors as in situ probes for staining of cells, tissues, and embryos. Methods Enzymol 2000;327:19-35.

32. Flanagan JG, Cheng HJ. Alkaline phosphatase fusion proteins for molecular characterization and cloning of receptors and their ligands. Methods Enzymol 2000;327:198-210.

33. Burfeind P, Chernicky CL, Rininsland F, Ilan J, Ilan J. Antisense RNA to the type I insulin-like growth factor receptor suppresses tumor growth and prevents invasion by rat prostate cancer cells in vivo. Proc Natl Acad Sci U S A 1996;93:7263-8.

34. Huang Y, Hoque MO, Wu F, Trink B, Sidransky D, Ratovitski EA. Midkine induces epithelial-mesenchymal transition through Notch2/Jak2-Stat3 signaling in human keratinocytes. Cell Cycle 2008;7:1613-22.

35. Güngör C, Zander H, Effenberger KE, Vashist YK, Kalinina T, Izbicki JR, et al. Notch Signaling Activated by Replication Stress-Induced Expression of Midkine Drives Epithelial-Mesenchymal Transition and Chemoresistance in Pancreatic Cancer. Cancer Res 2011;71:5009-19.

36. Muramatsu T. Protein-bound carbohydrates on cell-surface as targets of recognition: an odyssey in understanding them. Glycoconj J 2000;17:577-95.

37. Chen S, Bu G, Takei Y, Sakamoto K, Ikematsu S, Muramatsu T, et al. Midkine and LDL-receptor-related protein 1 contribute to the anchorage-independent cell growth of cancer cells. J Cell Sci 2007;120:4009-15.

38. Sakamoto K, Bu G, Chen S, Takei Y, Hibi K, Kodera Y, et al. Premature ligand-receptor interaction during biosynthesis limits the production of growth factor midkine and its receptor LDL receptor-related protein 1. J Biol Chem 2011;286:8405-13.

39. Maeda N, Ichihara-Tanaka K, Kimura T, Kadomatsu K, Muramatsu T, Noda M. A receptor-like protein-tyrosine phosphatase PTPζ/RPTPβ binds a heparin-binding growth factor midkine. Involvement of arginine 78 of midkine in the high affinity binding to PTPz. J Biol Chem 1999;274:12474-9.

40. Muramatsu H, Zou P, Suzuki H, Oda Y, Chen GY, Sakaguchi N, et al. α4β1- and α6β1-integrins are functional receptors for midkine, a heparin-binding growth factor. J Cell Sci 2004;117:5405-15.

41. Stoica GE, Kuo A, Powers C, Bowden ET, Sale EB, Riegel AT, et al. Midkine binds to anaplastic lymphoma kinase (ALK) and acts as a growth factor for different cell types. J Biol Chem 2002;277:35990-8.

42. Alam G, Cui H, Shi H, Yang L, Ding J, Mao L, et al. MYCN promotes the expansion of Phox2B-positive neuronal progenitors to drive neuroblastoma development. Am J Pathol 2009;175:856-66.

43. Keefe AD, Pai S, Ellington A. Aptamers as therapeutics. Nat Rev Drug Discov 2010;9:537-50.

44. Nakamura Y, Ishiguro A, Miyakawa S. RNA plasticity and selectivity applicable to therapeutics and novel biosensor development. Genes Cells 2012;17:344-64.

45. Mossé YP, Laudenslager M, Longo L, Cole KA, Wood A, Attiyeh EF, et al. Identification of ALK as a major familial neuroblastoma predisposition gene. Nature 2008;455:930-5.

46. Janoueix-Lerosey I, Lequin D, Brugières L, Ribeiro A, de Pontual L, Combaret V, et al. Somatic and germline activating mutations of the ALK kinase receptor in neuroblastoma. Nature 2008;455:967-70.

47. Chen Y, Takita J, Choi YL, Kato M, Ohira M, Sanada M, et al. Oncogenic mutations of ALK kinase in neuroblastoma. Nature 2008;455:971-4.

48. George RE, Sanda T, Hanna M, Fröhling S, Luther W 2nd, Zhang J, et al. Activating mutations in ALK provide a therapeutic target in neuroblastoma. Nature 2008;455:975-8.

49. Betancur P, Bronner-Fraser M, Sauka-Spengler T. Assembling neural crest regulatory circuits into a gene regulatory network. Annu Rev Cell Dev Biol 2010;26:581-603.

50. Reiff T, Huber L, Kramer M, Delattre O, Janoueix-Lerosey I, Rohrer H. Midkine and Alk signaling in sympathetic neuron proliferation and neuroblastoma predisposition. Development 2011;138:4699-708.

Figure Legends

Figure 1. MK is expressed in the precancerous lesions of MYCN Tg mice

A, H&E staining of SMG from wild-type or MYCN Tg mice (hemizygotes) at the age of 2 weeks. Arrowheads indicate the hyperplasia lesions. Lower pictures are magnifications of the boxed region in the upper pictures. Scale bar: 200 μm. B, RT-PCR with 2-week-old SMG. Six wild-type mice and five MYCN Tg mice (hemizygotes) were examined. C, Quantitative real-time PCR for MK with the same samples in B. *: $p<0.001$. D, SMG from 2-week-old MYCN Tg mice were immunostained with anti-MK antibody. Arrowheads indicate the hyperplasia lesions. Lower pictures are magnifications of the boxed region in the upper pictures. Scale bar: 200 μm. E, SMG from 2-week-old MYCN Tg mice were immunostained for each protein. Arrowheads indicate the hyperplasia lesions. Scale bar: 100 μm.

Figure 2. The suppression of tumor incidence and progression in MK-knockout mice

A, MYCN hemizygous mice with each MK genotype (+/+, +/- and -/-) were monitored for their tumor formations. 328 $MK^{+/+}$, 76 $MK^{+/-}$ and 186 $MK^{-/-}$ mice were examined. *: $p<0.01$. N.S.: not significant. B. MK protein levels in the tumor tissues from each MK genotype. Three terminal tumors from each MK genotype were subjected to Western blotting with anti-MK antibody.

Figure 3. Activation of Notch2 is diminished in the precancerous lesions of $MK^{-/-}$ mice

The 2-week-old SMG from $MK^{+/+}$ (A, B, C) or $MK^{-/-}$ (D, E, F) MYCN Tg (hemizygous) mice was subjected to immunohistochemistry with the full-length (FL) (A, D) or the intracellular domain (ICD) (B, E) of Notch2 and HES1 (C, F). Lower pictures are magnifications of the boxed region in the upper ones. Notch2 (ICD), an activated form, and HES1 were markedly diminished in $MK^{-/-}$ mice (E, F) compared to hemizygous $MK^{+/+}$ mice (B, C). Scale bar: 200 μm.

Figure 4. An RNA aptamer targeting MK inhibits its binding to the cell

surface

A, SPR assays showed that the RNA aptamer Apt-1 bound to MK but not to PTN and other plasma proteins. For the SPR assays, each RNA aptamer was bound to the surface of the sensor chip and 100 nM of each protein (MK, PTN, human IgG1 (hIgG1) and human serum albumin (HSA)) was injected. B, Preparation of AP-MK fusion protein. The media of 293T cells transfected with expression vectors were collected and used for the Western blotting with anti-AP or anti-MK antibodies. C, *in vitro* AP assay. TNB1 cells were treated with the AP-MK fusion protein in the presence of each aptamer, and the AP activity bound on the cell surface was measured. *: $p<0.001$. D, TNB1 cells were treated with 100 nM of aptamers for 24 hours, and Notch2 (ICD) and Histone H3 (internal control) were detected by Western blotting. E. The expression of HES1 mRNA was examined by real-time PCR using samples with the same condition as D. *: $p<0.05$.

Figure 5. The RNA aptamer Apt-1 suppressed the growth of TNB1 cells both *in vitro* and *in vivo*

A, Soft agar colony formation assay with RNA aptamers. Apt-1 efficiently inhibited the anchorage-independent growth of TNB1 cells. The addition of recombinant MK protein (100 ng/ml) could cancel the inhibitory effect of Apt-1. *: $p<0.001$. B, Soft agar assay with LNCap cells. Apt-1 could not suppress the colony formation of LNCap cells. C, Western blotting to detect secreted MK from each cell line. LNCap cells showed little MK expression. D, The experimental scheme for the RNA aptamer-mediated MK-targeting therapy with TNB1 xenograft tumors. E, Tumor growth curves (volume). *: $p<0.01$. F, Tumor weights at 3 weeks. *: $p<0.01$.

Figure 6. The attenuation of Notch2 signaling in Apt-1-treated TNB1 xenograft tumors

A, Immunohistochemistry of xenograft tumors with Notch2 (ICD) and HES1. Both Notch2 (ICD) and HES1 showed the attenuated signals in Apt-1-treated tumors. Scale bar: 50 μm. B, Western blotting to detect Notch2 (ICD) and phosphorylated ALK. 4 tumors for each condition were examined. Histone H3

and β-actin were internal controls for nucleus and cytosol & membrane fractions, respectively. C, Xenograft tumors were subjected to real-time PCR for HES1. *: $p<0.05$.

Author Manuscript Published OnlineFirst on December 14, 2012; DOI: 10.1158/0008-5472.CAN-12-3070
Author manuscripts have been peer reviewed and accepted for publication but have not yet been edited.

Figure 1.

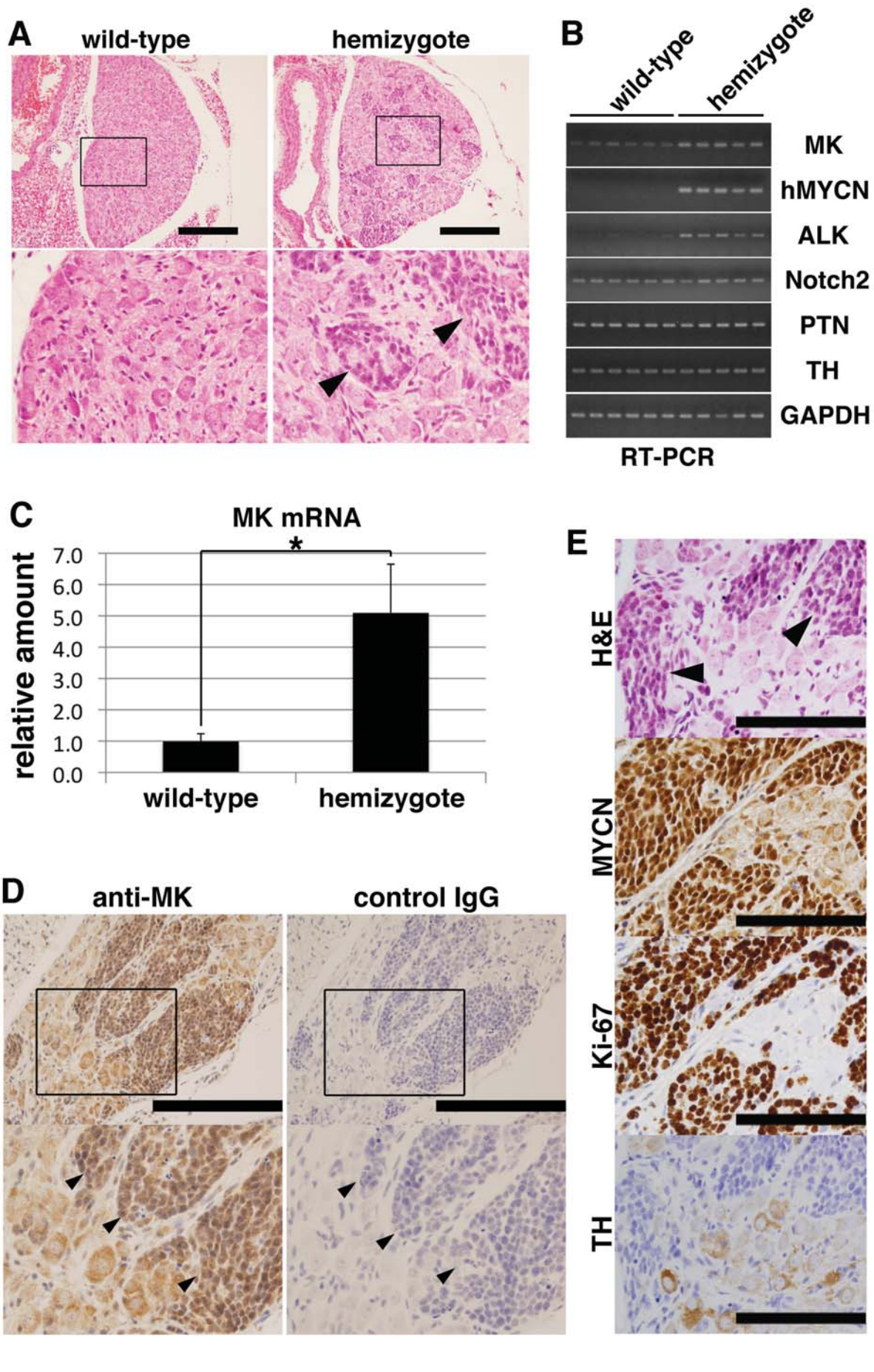

Author Manuscript Published OnlineFirst on December 14, 2012; DOI: 10.1158/0008-5472.CAN-12-3070
Author manuscripts have been peer reviewed and accepted for publication but have not yet been edited.

Figure 2.

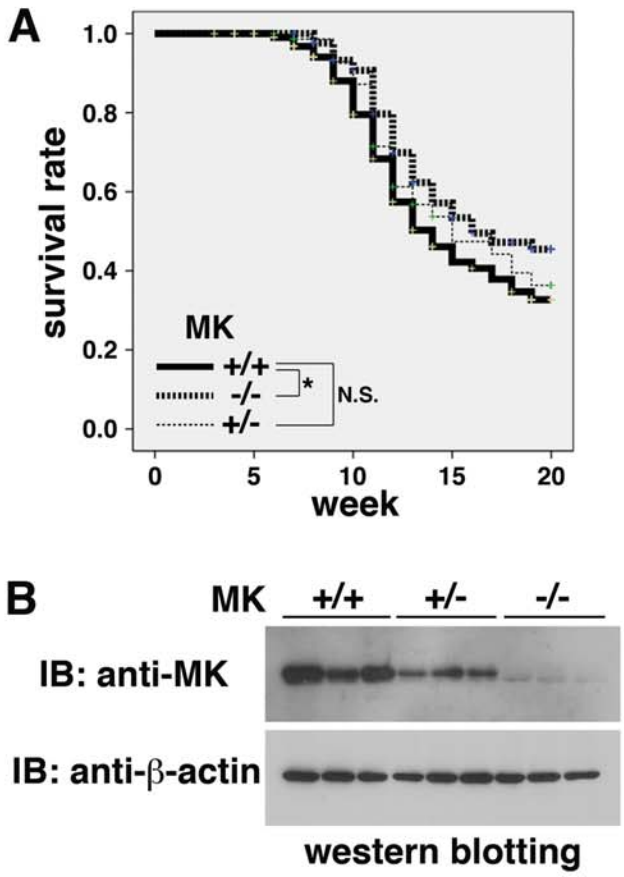

Author Manuscript Published OnlineFirst on December 14, 2012; DOI: 10.1158/0008-5472.CAN-12-3070
Author manuscripts have been peer reviewed and accepted for publication but have not yet been edited.

Figure 3.

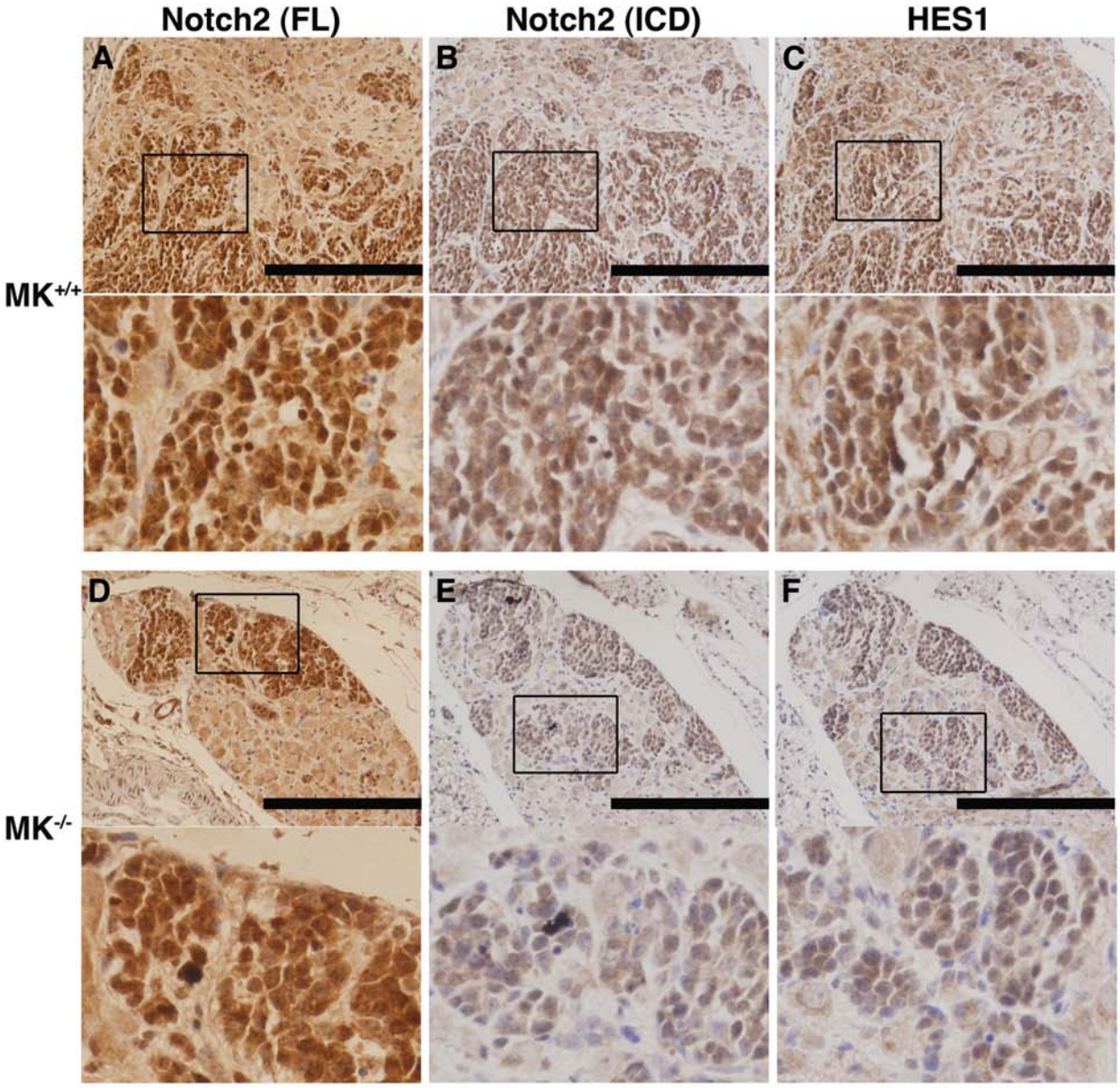

Author Manuscript Published OnlineFirst on December 14, 2012; DOI: 10.1158/0008-5472.CAN-12-3070
Author manuscripts have been peer reviewed and accepted for publication but have not yet been edited.

Figure 4.

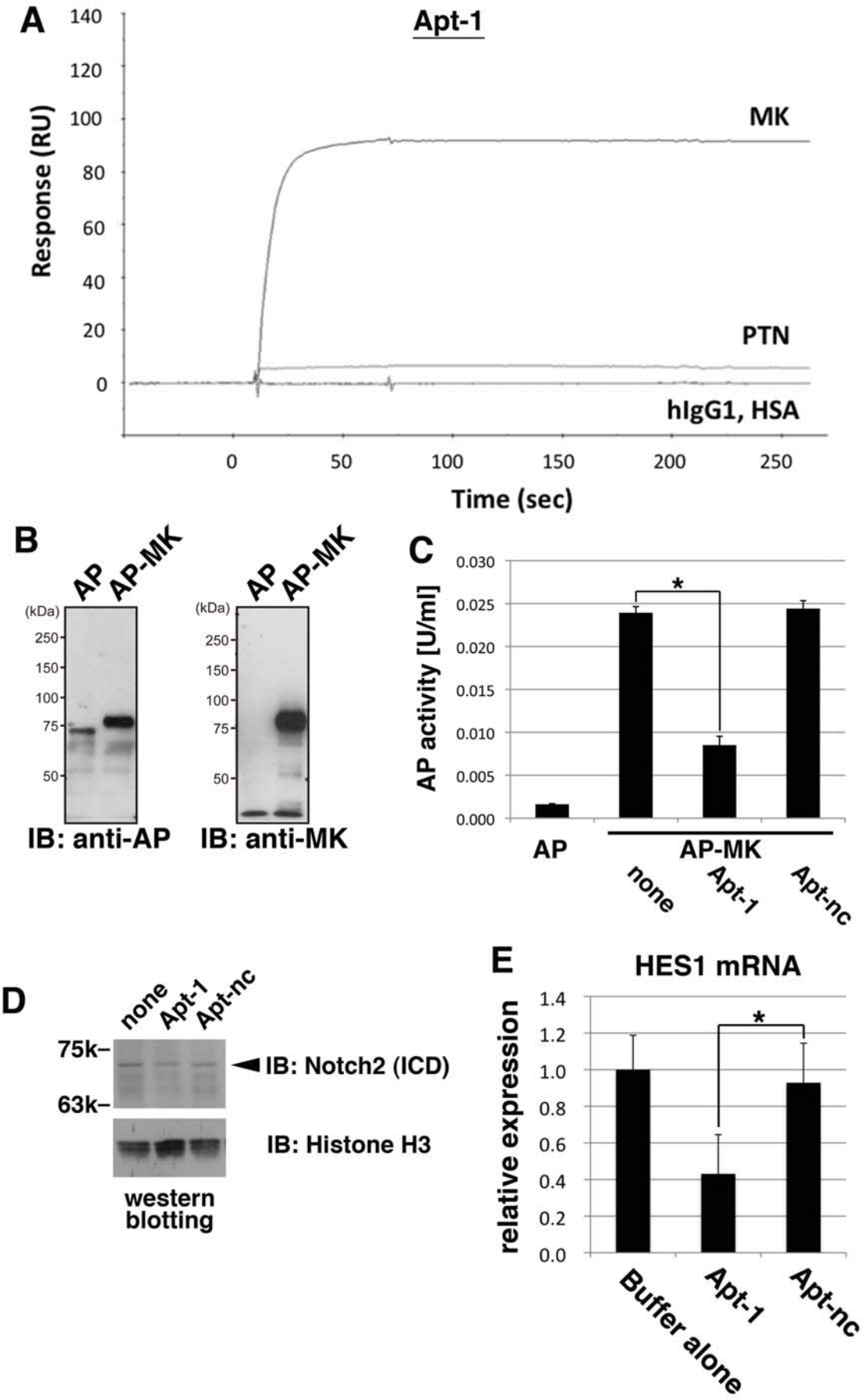

Author Manuscript Published OnlineFirst on December 14, 2012; DOI: 10.1158/0008-5472.CAN-12-3070
Author manuscripts have been peer reviewed and accepted for publication but have not yet been edited.

Figure 5.

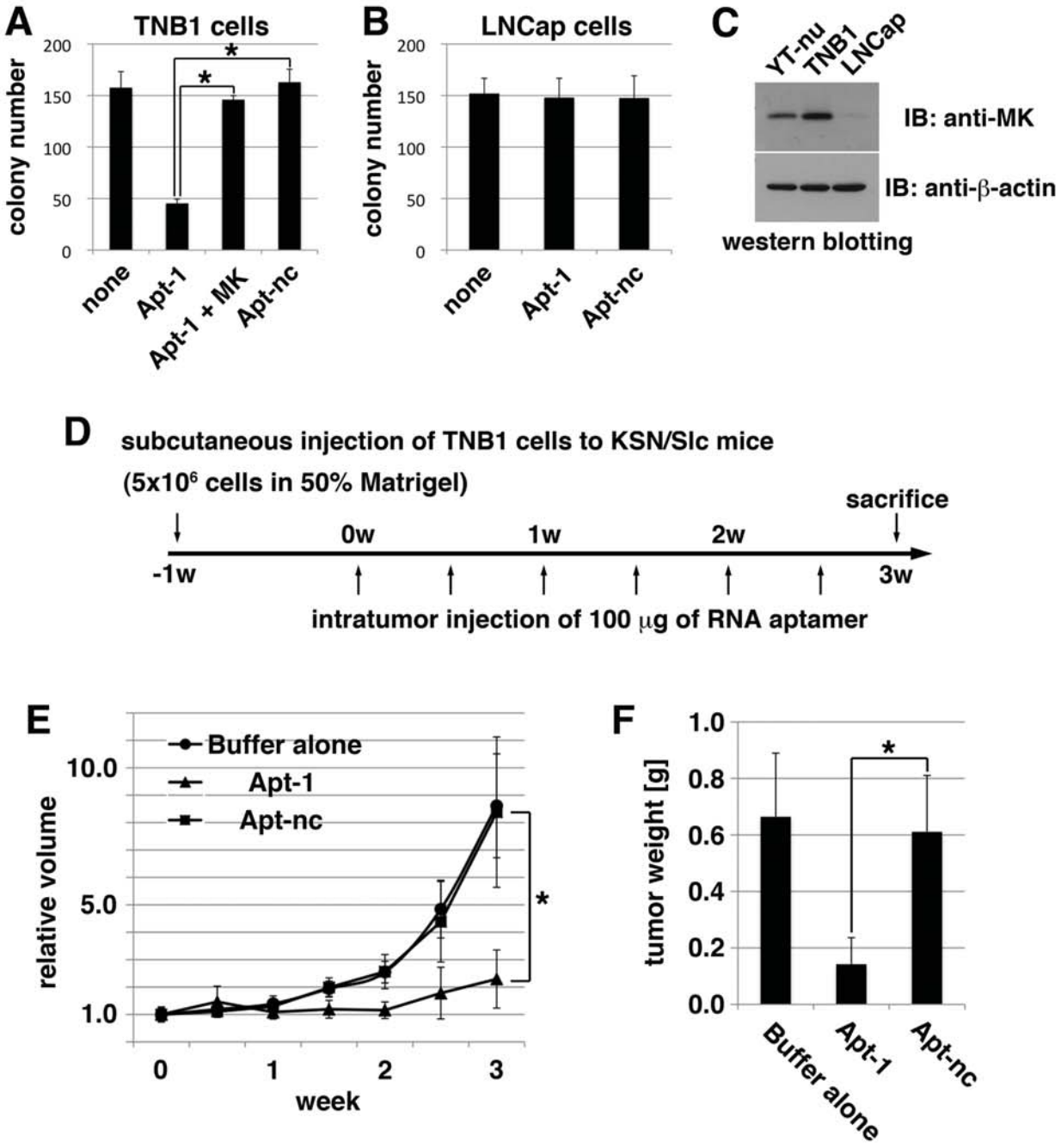

Author Manuscript Published OnlineFirst on December 14, 2012; DOI: 10.1158/0008-5472.CAN-12-3070
Author manuscripts have been peer reviewed and accepted for publication but have not yet been edited.

Figure 6.

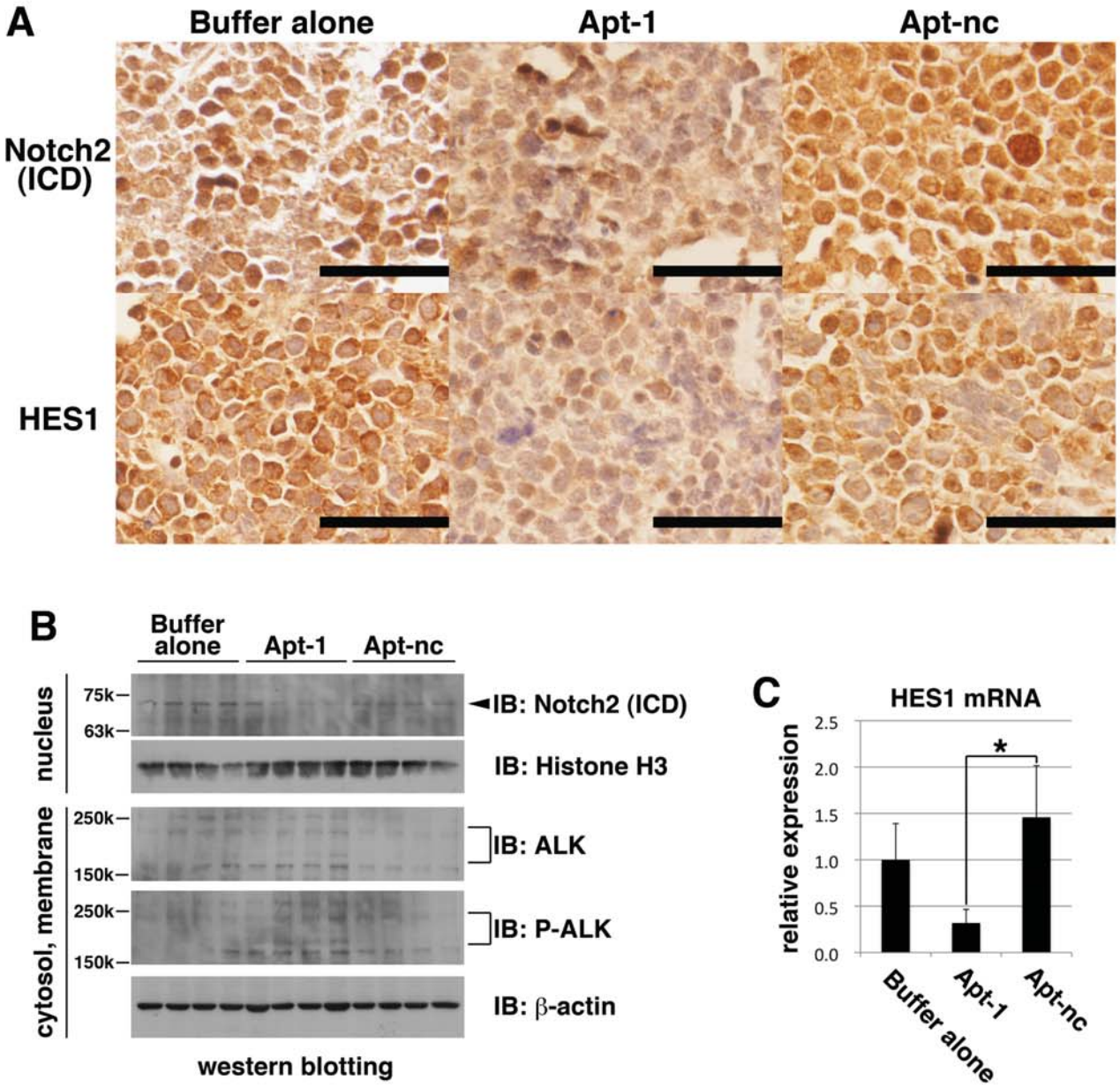

AACR American Association for Cancer Research

Cancer Research

The Journal of Cancer Research (1916–1930) | The American Journal of Cancer (1931–1940)

Midkine promotes neuroblastoma through Notch2 signaling

Satoshi Kishida, Ping Mu, Shin Miyakawa, et al.

Cancer Res Published OnlineFirst December 14, 2012.